Journal of Power Sources 189 (2009) 786–789

Contents lists available at ScienceDirect

Journal of Power Sources

journal homepage: www.elsevier.com/locate/jpowsour

Short communication

$LiVOPO_4$: A cathode material for 4 V lithium ion batteries

M.M. Ren, Z. Zhou*, L.W. Su, X.P. Gao

Institute of New Energy Material Chemistry, Nankai University, Tianjin 300071, China

ARTICLE INFO

Article history:
Received 12 June 2008
Received in revised form 22 July 2008
Accepted 31 July 2008
Available online 15 August 2008

Keywords:
Li ion batteries
Cathode material
β-$LiVOPO_4$
RuO_2

ABSTRACT

Electroactive lithium vanadyl phosphate, β-$LiVOPO_4$, was synthesized via a sol–gel route, and β-$LiVOPO_4$/RuO_2 composite was subsequently prepared by heating $RuCl_3$ in the network of β-$LiVOPO_4$ particles. X-ray diffraction patterns showed that β-$LiVOPO_4$ has an orthorhombic structure with space group of *Pnma*. Energy dispersive X-ray spectroscopy dot mappings revealed that ruthenium was homogeneously distributed among β-$LiVOPO_4$ particles. Compared with pristine β-$LiVOPO_4$, β-$LiVOPO_4$/RuO_2 composite presented better electrochemical Li ion intercalation performances due to the enhanced electrical conductivity and Li ion diffusion. β-$LiVOPO_4$ may be prospective for the application to high-voltage Li ion batteries if the electrical conductivity is improved through a practical way.

1. Introduction

Nowadays Li ion batteries have been widely used in many fields as power suppliers for mobile equipment. The present commercial cathode material, $LiCoO_2$, possesses some problems in large-scale utilization, due to the high cost and safety. Transition metal phosphates have been attracting much interest as a new class of cathode materials for Li ion batteries, such as $LiMPO_4$ (M=Fe, Mn, or Co) [1–4], $Li_3V_2(PO_4)_3$ [5–10], and $LiVPO_4F$ [11,12]. These materials contain both mobile Li ions and redox-active transition metals within a rigid phosphate network, and display remarkable electrochemical and thermal stability as well as comparable energy density. One of the main drawbacks in these materials is their poor electrical conductivity [13,14]. Low electrical conductivity affects the migration kinetics of Li^+ ions and electrons during electrochemical reaction [15], and therefore influences the charge/discharge capacities especially when the electrodes are tested at high rates.

In search for ideal polyanion insertion hosts, lithium vanadyl phosphate ($LiVOPO_4$) is also a candidate [16–22]. $LiVOPO_4$ contains two crystal phases, α- and β-$LiVOPO_4$. α-$LiVOPO_4$ is triclinic structure (space group $P\bar{1}$), and β-$LiVOPO_4$ is orthorhombic structure (space group *Pnma*) [17,19]. α-$LiVOPO_4$ has ever been synthesized via a sol–gel [23] and one-pot hydrothermal route [24]; however, this material showed rather poor electrochemical performances. Barker et al. synthesized β-$LiVOPO_4$ through a carbothermal reaction, and the V^{4+}/V^{5+} redox transition in β-$LiVOPO_4$ was located around 3.9 V vs. Li^+/Li [17]. Azmi et al. prepared β-$LiVOPO_4$ through solid-state reactions, and its electrochemical performances were also poor [20]. β-$LiVOPO_4$ has the theoretical specific capacity of ~166 mAh g^{-1}, as high as $LiFePO_4$. Compared with $LiFePO_4$, this cathode material has higher charge/discharge plateau (around 4.0 V). In addition, contrast with $Li_3V_2(PO_4)_3$ which has the highest theoretical specific capacity (197 mAh g^{-1}) among the transition metal phosphates, β-$LiVOPO_4$ has only one charge/discharge plateau, which can help its utilization in practical lithium ion batteries. However, due to the low electrical conductivity and Li ion diffusion, the electrochemical performance of this cathode material is still poor. It was regarded that this problem could be solved to some degree by mixing with electrically conducting materials; however, our experimental results showed that the simple addition of carbon did not lead to apparent enhancement in electrochemical performances. Since it is reported that RuO_2 remarkably increased the electrical conductivity and electrochemical performances of some Li ion battery materials [15,25,26], in this work β-$LiVOPO_4$/RuO_2 composite was investigated to explore whether β-$LiVOPO_4$ is prospective in high-voltage Li ion batteries on condition that the low electrical conductivity problem is completely resolved. Though we know that RuO_2 is rather expensive for practical applications, the results and mechanism revealed in this work are useful for the future improvement of this material.

2. Experimental

2.1. Sample preparation

β-$LiVOPO_4$ was synthesized through a sol–gel route. Starting materials were V_2O_5, $LiNO_3{\cdot}6H_2O$, $NH_4H_2PO_4$ and oxalic acid. Firstly, oxalic acid and V_2O_5 in stoichiometric ratio were dissolved

* Corresponding author. Tel.: +86 22 23498941; fax: +86 22 23498941.
E-mail address: zhouzhen@nankai.edu.cn (Z. Zhou).

0378-7753/$ – see front matter © 2008 Elsevier B.V. All rights reserved.
doi:10.1016/j.jpowsour.2008.07.092

in deionized water with magnetic stirring at 70 °C (Eq. (1)). After a clear blue solution formed, a mixture of stoichiometric $NH_4H_2PO_4$ and $LiNO_3{\cdot}6H_2O$ was added to the solution while stirring for 4 h, and then a gel formed in an air oven at 100 °C. Finally, the gel was decomposed at 300 °C for 4 h, and the obtained product was sintered at 500 °C for 4 h in air (Eq. (2)). β-$LiVOPO_4$/RuO_2 composite was prepared as follows; 500 mg of β-$LiVOPO_4$ was soaked by 4 ml of 0.05 mol l^{-1} $RuCl_3$ solution, and after drying at 50 °C, the powder was calcined at 450 °C for 1 h in air (Eq. (3)), and the weight ratio of RuO_2 in the $LiVOPO_4$/RuO_2 composite is about 5%.

$$V_2O_5 + 3H_2C_2O_4 \rightarrow 2VOC_2O_4 + 3H_2O + 2CO_2 \quad (1)$$

$$VOC_2O_4 + LiNO_3 + NH_4H_2PO_4 \rightarrow LiVOPO_4 + 2CO + 2NO + 3H_2O \quad (2)$$

$$RuCl_3 + 1/4O_2 + 3/2H_2O \rightarrow RuO_2 + 3HCl \quad (3)$$

2.2. Sample characterization

X-ray diffraction (XRD) patterns of the samples were measured using the D/MAX III diffractometer with Cu Kα radiation (λ = 1.5418 Å). A JEOL-7500F scanning electron microscopy (SEM) was used to investigate the morphology of the samples. The electrical conductivities of the samples were measured by linear potential scan within a Zahner-Elektrik IM6e electrochemical workstation. The pristine β-$LiVOPO_4$ and β-$LiVOPO_4$/RuO_2 pellets used for electrical conductivity measurements were prepared by uniaxially pressing the powders with a pressure of 10 MPa, and then Ag paste was coated on both sides of the pellets of about 13 mm in diameter and 1.3 mm in thickness.

2.3. Galvanostatic charge/discharge tests

Electrochemical Li ion intercalation performances of the samples were evaluated in Li test cells. The cathode materials were prepared by mixing the samples with acetylene black and polytetrafluoroethylene (PTFE) with a weight ratio of 75:20:5 in ethanol to ensure homogeneity. After the ethanol was evaporated, the mixture was rolled into a sheet, and the sheet was cut into circular strips of 8 mm in diameter. The strips were then dried at 100 °C for 10 h. Lithium metal was used as an anode. The electrolyte was composed of a 1 mol l^{-1} $LiPF_6$ dissolved in ethylene carbonate (EC)/dimethyl carbonate (DMC)/ethylene methyl carbonate (EMC) with the volume ratio of 1:1:1. Test cells were assembled in an argon-filled dry glove box. The galvanostatic charge/discharge tests were performed within a Land CT2001 battery tester at different current densities in a voltage range of 3.0–4.5 V at 25 °C.

2.4. CV measurements

Cyclic voltammograms (CVs) were conducted within a LK2005A electrochemical workstation. The CV curves were recorded for the above test cells in a potential range of 3.0–4.5 V (vs. Li^+/Li) with different scan rates at 25 °C.

3. Results and discussion

3.1. Sample characterization

Fig. 1 shows the XRD patterns of pristine β-$LiVOPO_4$ and β-$LiVOPO_4$/RuO_2 composite. β-$LiVOPO_4$ possesses an orthorhombic symmetry with space group *Pnma*. There are two impurity peaks

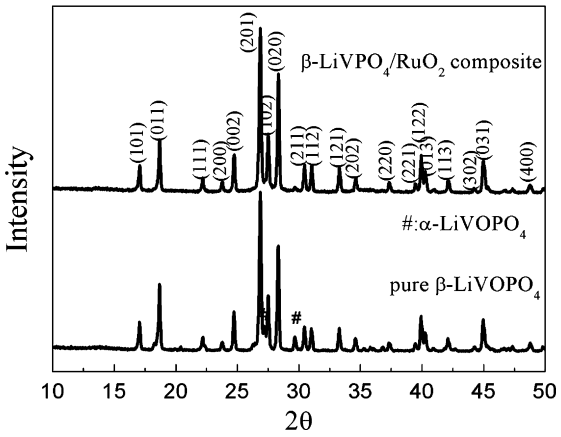

Fig. 1. X-ray diffraction patterns of pristine β-$LiVOPO_4$ and β-$LiVOPO_4$/RuO_2 composite.

at 27.2° and 29.7°, which are ascribed to α-$LiVOPO_4$. The reflections from β-$LiVOPO_4$/RuO_2 composite are indexed with JCPDS (No. 85-2438). RuO_2 is not detected from the XRD patterns, since the strongest peak indexed as (1 1 0) of RuO_2 (JCPDS No. 40-1290) overlaps with that of (0 2 0) of β-$LiVOPO_4$. Accordingly, in Fig. 1 the intensity ratio of (0 2 0) vs. (2 0 1) increases from 0.66 for pristine β-$LiVOPO_4$ to 0.72 for β-$LiVOPO_4$/RuO_2 composite, indicating the existence of RuO_2 in β-$LiVOPO_4$/RuO_2 composite. The result can also be confirmed by the following Energy dispersive spectroscopy (EDS) analysis.

The SEM image of β-$LiVOPO_4$/RuO_2 composite and the corresponding EDS dot mappings of Ru and V are shown in Fig. 2. The SEM image (Fig. 2a) shows that the sample consists of uniform particles with average sizes of ~2 μm. The EDS dot mappings reveal that Ru is homogeneously distributed among β-$LiVOPO_4$ particles.

The electrical conductivities of pristine β-$LiVOPO_4$ and β-$LiVOPO_4$/RuO_2 composite are 1.42×10^{-8} and 2.65×10^{-6} S cm^{-1}, respectively. As RuO_2 is metallic, the three-dimensional (3D) interconnected network among β-$LiVOPO_4$ particles enhanced the electronic conduction of the sample [15,27].

3.2. Galvanostatic charge/discharge tests

The electrochemical performances of β-$LiVOPO_4$ are increased significantly due to the coexistence of RuO_2 network. Fig. 3 shows the fifth-cycle charge/discharge profile of pristine β-$LiVOPO_4$ and β-$LiVOPO_4$/RuO_2 composite measured at the current density of 10 mA g^{-1} in the potential range of 3.0–4.5 V at 25 °C. Both electrodes exhibit the charge plateau around 4.04 V and a corresponding discharge plateau around 3.95 V; the discharge capacities of pristine β-$LiVOPO_4$ and β-$LiVOPO_4$/RuO_2 composite are 91.6 and 118.6 mAh g^{-1}, respectively.

The effect of RuO_2 can be seen more significantly from the long-term cyclic charge/discharge tested at higher current density, as shown in Fig. 4. The discharge capacity of β-$LiVOPO_4$/RuO_2 composite is 118.6 mAh g^{-1} after 30 cycles at the current density of 10 mA g^{-1}, much higher than that of pristine β-$LiVOPO_4$ (77.7 mAh g^{-1}); therefore, the retention rate in discharge capacities is ~100% for β-$LiVOPO_4$/RuO_2 composite after 30 cycles, but only 82.9% for pristine β-$LiVOPO_4$. Even at the higher current density of 80 mA g^{-1}, β-$LiVOPO_4$/RuO_2 composite shows higher discharge capacity than that of pristine β-$LiVOPO_4$ tested at the current density of 10 mA g^{-1}; after 30 cycles the discharge capacity retains 86 mAh g^{-1}, and the retention rate still attains 96.2%. Therefore, the charge/discharge capacity and cyclic stability of β-$LiVOPO_4$ are apparently improved as a result of the introduction of

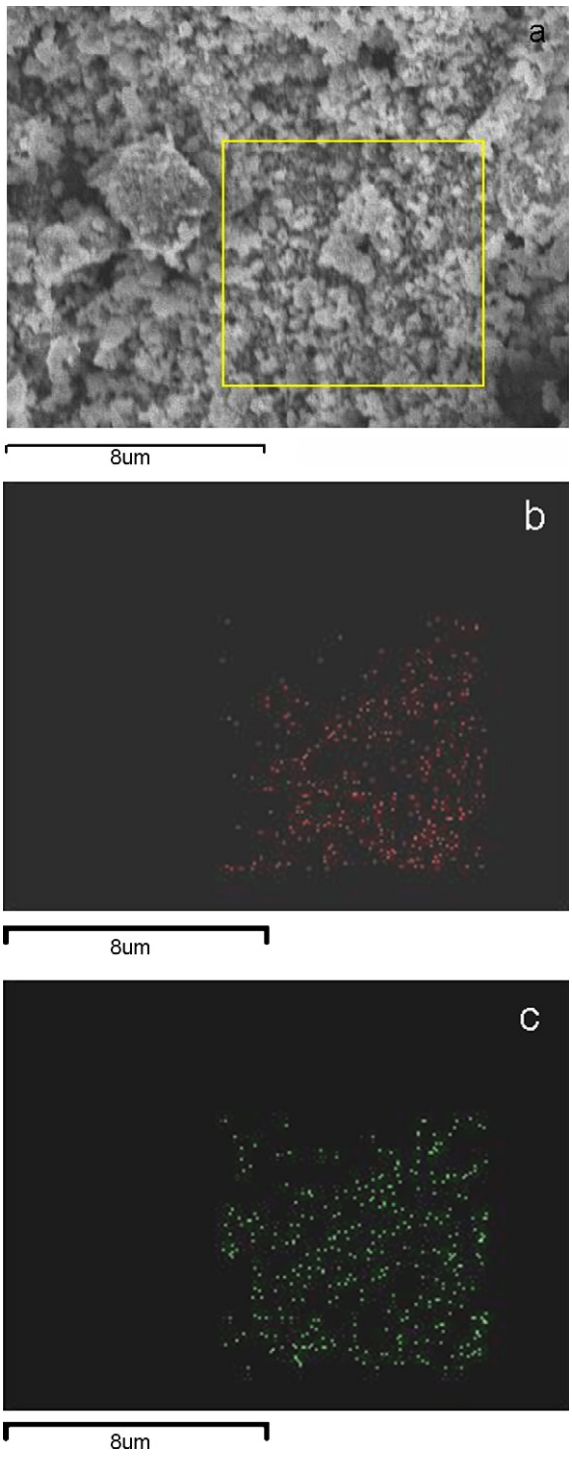

Fig. 2. SEM image of β-$LiVOPO_4$/RuO_2 composite (a) and the corresponding EDS dot mapping of (b) Ru and (c) V in the surface of β-$LiVOPO_4$/RuO_2.

RuO_2 network. Both samples exhibited that the discharge capacities increased during the initial cycles, since there was an activation process necessary for this material.

3.3. CV measurement

The initial CV curves are shown in Fig. 5 for pristine β-$LiVOPO_4$ and β-$LiVOPO_4$/RuO_2 composite. The oxidation peak is located around 4.11 V and the reduction peak is located around 3.86 V in

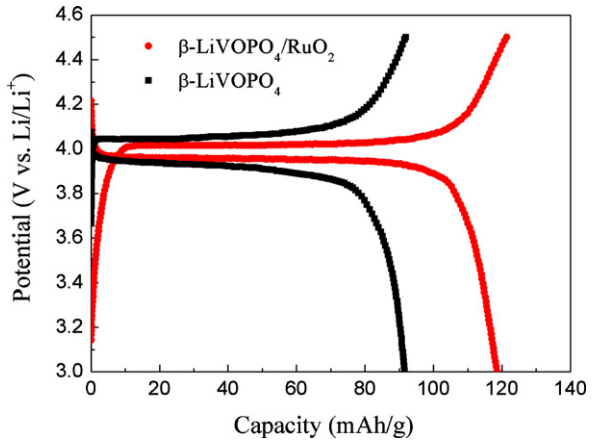

Fig. 3. The fifth charge/discharge curves of pristine β-$LiVOPO_4$ and β-$LiVOPO_4$/RuO_2 composite.

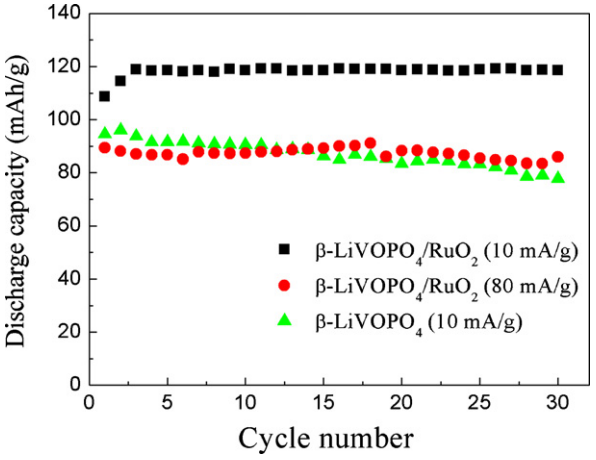

Fig. 4. Cyclic performance of pristine β-$LiVOPO_4$ and β-$LiVOPO_4$/RuO_2 composite electrodes tested at different current densities at 25 °C.

the potential range of 3.0–4.5 V for both electrodes, in agreement with the charge/discharge curves (Fig. 3). The anodic peak corresponds to the removal of Li from the framework of β-$LiVOPO_4$, and the cathodic peak is attributed to the re-insertion of Li ions.

Some difference can be seen from the CV curves. Firstly, the current density of the β-$LiVOPO_4$/RuO_2 composite electrode is higher than that of pure β-$LiVOPO_4$ electrode. For the coin-type

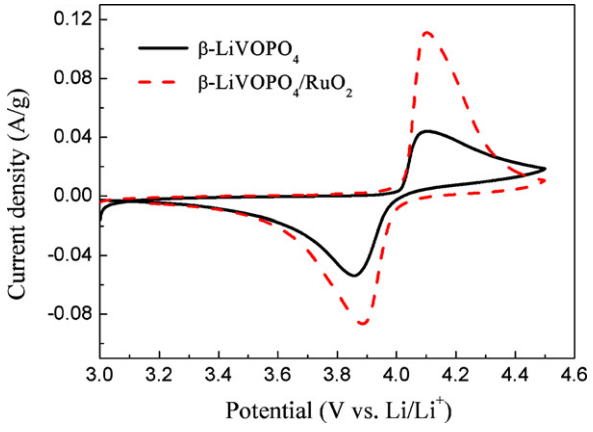

Fig. 5. CV curves of the first cycle for pristine β-$LiVOPO_4$ and β-$LiVOPO_4$/RuO_2 composite electrodes at the scan rate of 0.05 mV s^{-1}.

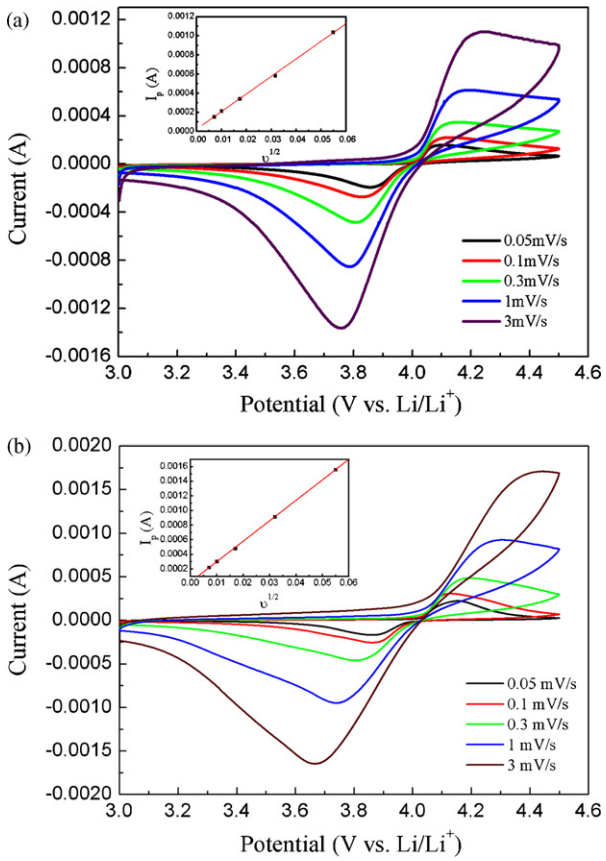

Fig. 6. CV curves for pristine β-LiVOPO$_4$ (a) and β-LiVOPO$_4$/RuO$_2$ composite (b) electrodes at different scan rates (0.05, 0.1, 0.3, 1, and 3 mV s^{-1}). The inset shows the relationship between the peak current and the scan rate.

Table 1
Potential difference between the anodic and cathodic peaks for β-LiVOPO$_4$ and β-LiVOPO$_4$/RuO$_2$ electrode

	E_{anodic} (V)	$E_{cathodic}$ (V)	E_{a-c} (V)
β-LiVOPO$_4$/RuO$_2$	4.101	3.889	0.212
β-LiVOPO$_4$	4.097	3.854	0.243

cell systems the electrodes can approximately be regarded as a flat one, and the peak current density is represented as follows; $i_p = 2.6 \times 10^5 n^{3/2} C_0 D^{1/2} A \nu^{1/2}$, where n is the number of electrons transferred per molecule during the intercalation, C_0 is the concentration of lithium ions, D is the diffusion coefficient of lithium ions, ν is the scan rate, and A is the surface area of the electrode [28,29]. Since $i_p \propto D^{1/2}$, as shown in Fig. 6, the diffusion coefficient of Li ions is higher in the β-LiVOPO$_4$/RuO$_2$ composite electrode than in the pure β-LiVOPO$_4$ electrode. The Li ion diffusion coefficients for the pure β-LiVOPO$_4$ electrode and β-LiVOPO$_4$/RuO$_2$ composite electrode are 1.20×10^{-11} and 2.79×10^{-11} cm^2 s^{-1}, respectively. Secondly, as summarized in Table 1, the potential difference between anodic and cathodic peaks is smaller in the β-LiVOPO$_4$/RuO$_2$ composite electrode. These results indicate that the kinetic for β-LiVOPO$_4$/RuO$_2$ composite is indeed improved, which is similar to the report on LiFePO$_4$/RuO$_2$ composite [27].

In the present work, metallic RuO$_2$ provides a 3D network for β-LiVOPO$_4$ particles; therefore, the insertion/extraction kinetics in β-LiVOPO$_4$ was improved, and then the electrochemical performances were increased accordingly. However, Ru is rare and expensive, and it is apparent that β-LiVOPO$_4$/RuO$_2$ composite is not practical for Li ion batteries. According to the results in this work, if the problem of electrical conductivity is completely solved, β-LiVOPO$_4$ may be prospective in 4 V Li ion batteries. Other cheap and effective methods are still necessarily exploited to improve the electrical conductivity of β-LiVOPO$_4$.

4. Conclusion

β-LiVOPO$_4$/RuO$_2$ composite was synthesized via a sol–gel route and a subsequent heat treatment. Energy dispersive X-ray spectroscopy dot mappings revealed that ruthenium was homogeneously distributed among β-LiVOPO$_4$ particles. Electrical conductivity and lithium ion diffusion were increased due to the existence of RuO$_2$. β-LiVOPO$_4$/RuO$_2$ composite exhibited enhanced discharge capacity and cyclic stability. The initial discharge capacity of β-LiVOPO$_4$/RuO$_2$ composite was 108.6 mAh g^{-1}, and in the 30th cycle it was 118.6 mAh g^{-1} at the current density of 10 mA g^{-1}, so the retention rate of discharge capacities was ~100%, much higher than that of pure β-LiVOPO$_4$. Even at higher current density (80 mA g^{-1}), the retention rate still reached 96.2% for β-LiVOPO$_4$/RuO$_2$ composite. RuO$_2$ network provided an effective way for the improvement of β-LiVOPO$_4$.

Acknowledgements

This work was supported by the 863 National High Technology Research and Development Program (2007AA03Z225), the 973 National Basic Research Program (2009CB220100), and Tianjin Natural Science Foundation (06YFJMJC13300) in China.

References

[1] A.K. Padhi, K.S. Najundaswamy, J.B. Goodenough, J. Electrochem. Soc. 144 (1997) 1118.
[2] A. Yamada, S.C. Chung, J. Electrochem. Soc. 148 (2001) A960.
[3] K. Amine, K. Yamachi, M. Yamachi, Electrochem. Solid State Lett. 3 (2000) A178.
[4] G. Azuma, H. Li, M. Tohdam, Electrochem. Solid State Lett. 5 (2002) A135.
[5] M.Y. Saidi, J. Barker, H. Huang, J.L. Sowyer, G.J. Adamson, J. Power Sources 119–112 (2003) 266.
[6] S.C. Yin, H. Grond, P. Strobel, H. Huang, L.F. Nazar, J. Am. Chem. Soc. 125 (2003) 326.
[7] H. Hung, S.C. Yin, T. Kerr, N. Taylor, L.F. Nazar, Adv. Mater. 14 (2002) 1525.
[8] M.M. Ren, Z. Zhou, Y.Z. Li, X.P. Gao, J. Yan, J. Power Sources 162 (2006) 1357.
[9] Y.Z. Li, Z. Zhou, M.M. Ren, X.P. Gao, J. Yan, Electrochim. Acta 51 (2006) 6498.
[10] M.M. Ren, Z. Zhou, X.P. Gao, W.X. Peng, J. Phys. Chem. C 112 (2008) 5689.
[11] J. Barker, M.Y. Saidi, J.L. Swoyer, J. Electrochem. Soc. 150 (2003) A1394.
[12] Y.Z. Li, Z. Zhou, X.P. Gao, J. Yan, J. Power Sources 160 (2006) 633.
[13] S.-Y. Chung, J.T. Bloking, Y.-M. Chiang, Nat. Mater. 1 (2002) 123.
[14] J.-M. Tarascon, M. Armand, Nature 414 (2001) 359.
[15] Y.G. Guo, Y.S. Hu, W. Sigle, J. Maier, Adv. Mater. 19 (2007) 2087.
[16] J. Ganbicher, T.L. Mercier, Y. Chahre, J. Angenault, M. Quarton, J. Electrochem. Soc. 146 (1999) 4375.
[17] J. Barker, M.Y. Saidi, J.L. Swoyer, J. Electrochem. Soc. 151 (2004) A796.
[18] B.M. Azmi, T. Ishihara, H. Nishiguchi, H. Nishiguchi, Y. Takita, Electrochem. Acta 48 (2002) 165.
[19] T.A. Kerr, J. Gaubicher, L.F. Nazar, Electrochem. Solid State Lett. 3 (2000) 460.
[20] B.M. Azmi, T. Ishihara, H. Nishiguchi, Y. Takita, J. Power Sources 146 (2005) 525.
[21] N. Dupre, J. Gaubicher, T.L. Mercier, G. Wallez, J. Angenault, M. Quarton, Solid State Ionics 140 (2001) 209.
[22] S.C. Lim, J.T. Vaughey, W.T.A. Harrison, L.L. Dussack, A.J. Jacobson, Solid State Ionics 84 (1996) 219.
[23] Y. Yong, H.S. Fang, J. Zheng, L.P. Li, G.S. Li, G.F. Yan, Solid State Sci. 10 (2008) 1292.
[24] M.M. Ren, Z. Zhou, X.P. Gao, L. Liu, W.X. Peng, J. Phys. Chem. C 112 (2008) 13043.
[25] P. Balaya, H. Li, L. Kienle, J. Maier, Adv. Funct. Mater. 13 (2003) 621.
[26] M. Armand, F. Dalard, D. Deroo, C. Mouliom, Solid State Ionics 15 (1985) 205.
[27] Y.S. Hu, Y.G. Guo, R. Dominko, M. Gaberscek, J. Jamnik, J. Maier, Adv. Mater. 19 (2007) 1963.
[28] H. Liu, L.J. Fu, H.P. Zhang, J. Gao, C. Li, Y.P. Wu, H.Q. Wu, Electrochem. Solid State Lett. 9 (2006) A529.
[29] A.J. Bard, L.R. Faulkner, Electrochemical Methods, Wiley, New York, 1980, p. 213.